

Supporting Information

Materials: Acrylamide (AM, $\geq 99\%$, AR,) , dodecyl methacrylate (LMA, $\geq 99\%$, RG), cetyltrimethylammonium Bromide (CTAB, 99% , RG) , $\text{ZnSO}_4 \cdot 7\text{H}_2\text{O}$ (AR, 99%) , MnSO_4 (AR, 99%) , 2-hydroxy-4'-(2-hydroxyethoxy)-2-methyl-propiophe (AR, 99%), N,N'-Methylenbisacrylamide (MBA, 99%, AR), manganese acetate tetrahydrate ($\text{Mn}(\text{CH}_3\text{COO})_2 \cdot 4\text{H}_2\text{O}$, RG $\geq 98\%$) , potassium permanganate (KMnO_4 , AR, $> 99\%$), N-methyl-pyrrolidone (NMP, AR, $\geq 99\%$), Carboxylic multi-walled carbon nanotubes were purchased from Shanghai Maclin Biochemical Technology Co., Ltd.

Preparation of hydrogel electrolyte: The preparation of LA gel electrolyte was carried out using a one-pot method. Initially, 0.5g of CTAB was dissolved in 3.74ml of deionized water, followed by the addition of varying masses of LMA (0.1g, 0.15g, 0.2g) with stirring for 2 hours. Subsequently, 1g of AM monomer, 2M ZnSO_4 , 0.1 MnSO_4 , and 10mg of 2-hydroxy-4'-(2-hydroxyethoxy)-2-methyl-propiophe were sequentially added and thoroughly mixed to obtain a homogeneous solution. After degassing, the precursor solution was transferred into a 1mm-thick mold and photoinitiated for 1 hour to yield the LA hydrogel electrolyte. Following the aforementioned steps, the pure PAM gel electrolyte without LMA and CTAB was synthesized, with the additional incorporation of 1mg of MBA as a crosslinking agent.

Preparation of MnO_2/CNT Cathode: The fabrication of MnO_2/CNT cathode: A hydrothermal method was employed to synthesize the MnO_2/CNT composite material. 0.15g of Carboxylic multi-walled carbon nanotubes were dispersed in 150ml of deionized water. Subsequently, 2.94g of $\text{Mn}(\text{CH}_3\text{COO})_2 \cdot 4\text{H}_2\text{O}$ was added and stirred continuously for 30 minutes. Thereafter, a KMnO_4 mixed solution, prepared by dispersing 1.27g of KMnO_4 in 80ml of deionized water, was slowly dripped into the aforementioned solution and stirred for an additional 30 minutes. The mixed solution

was then transferred into a Teflon-lined autoclave and maintained at 120°C for 12 hours. Finally, the resulting product was centrifuged and washed three times with deionized water, followed by drying in a vacuum oven at 80°C for 12 hours to obtain the MnO₂/CNT composite material. The MnO₂/CNT composite, Super P, and PVDF were mixed in a weight ratio of 7:2:1 in N-methyl-2-pyrrolidone (NMP). The slurry was then coated onto a titanium foil and dried at 80°C for 12 hours to yield the MnO₂/CNT cathode. The loading of MnO₂/CNT was approximately 1-1.5mg cm⁻².

Materials characterizations: The gaseous products were analyzed using gas chromatography (Agilent Technologies-7890B). X-ray diffraction (XRD) patterns were obtained on a desktop X-ray diffractometer (RIGAKU-Miniflex II) with Cu K α radiation ($\lambda = 1.5406 \text{ \AA}$) over a 2θ range of 3-80°. Nuclear magnetic resonance (NMR) spectroscopy was conducted on an AVANCE NEO 600 operating at 600 MHz. Raman spectroscopy of the samples was acquired using a DXR2Xi with a laser wavelength of 532 nm. The structure of the hydrogel was analyzed using a Fourier-transform infrared spectrometer (Nicolet 5700) with a wavenumber range of 400-4000 cm⁻¹. The morphology of the samples was characterized using a field-emission scanning electron microscope (SEM) JEOL JSM-7500F with an accelerating voltage of 3.0 kV. The mechanical properties of the samples were characterized using a universal tensile testing machine.

Electrochemical measurements: CR2032 coin cells were assembled under ambient atmosphere conditions. The LA gel was cut into a 16mm diameter disc to serve as the hydrogel electrolyte. When using a liquid electrolyte (2M aqueous solution of ZnSO₄), a glass fiber separator (Whatman, GF/D, 16mm in diameter) was employed. The zinc foil had a diameter of 12mm, and the copper foil had a diameter of 16mm. The cells were assembled into Zn||Zn, Zn||Cu, Zn||SS, and Zn||MnO₂/CNT batteries, respectively. The aforementioned batteries were tested using a Neware (CT-4800) battery cycle system. The charging cut-off voltage window for the Zn||MnO₂/CNT battery was set to 0.8-1.8V. Cyclic voltammetry (CV), linear sweep voltammetry (LSV),

chronoamperometry (CA), and electrochemical impedance spectroscopy (EIS) were conducted on a CHI660E electrochemical workstation. The EIS measurements were performed over a frequency range of 100 kHz to 0.01 Hz with an amplitude perturbation of 10 mV. LSV tests were carried out using Zn and Ti as the reference and working electrodes, respectively, at a scan rate of 1 mV/s, ranging from the original potential to 3.0 V and from the original potential to -0.5 V. Tafel tests were performed within a three-electrode setup, with zinc, platinum, and Ag/AgCl serving as the working, counter, and reference electrodes, respectively, at a scan rate of 5 mV/s.

The ionic conductivity of the electrolyte is calculated using the bulk resistance, which is measured on a Zahner-Zennium electrochemical workstation. The AC voltage amplitude is set to 5mV, and the frequency range is from 100 kHz to 1 Hz. The ionic conductivity (σ) was calculated by:

$$\sigma = \frac{D}{RA}$$

D, R, and A represent the thickness, bulk resistance, and testing area of the electrolyte, respectively.

The de-solvation energy (E_a) was determined by measuring the impedance variation under different temperatures and then fitting the data according to the Arrhenius equation:

$$\frac{1}{R_{ct}} = Ae^{-\left(\frac{E_a}{RT}\right)}$$

where R_{ct} represents the charge transfer resistance, A is the pre-exponential factor, R is the molar gas constant, and T denotes the absolute temperature.

Computation Method: The Density functional theory (DFT) calculations were performed using the Gaussian and VASP programs. Structure optimizations were carried out at the B3LYP-6-311++G** level and Vienna ab initio simulation package (VASP)

The energy (ΔE) of binding energy and adsorption energy is defined as follows:

$$\Delta E = E_{AB} - E_A - E_B$$

AI-MD simulations were conducted using the MD software CP2K. The initial box size was set to $20 \times 20 \times 20$ Å with periodic boundary conditions applied in all three directions. The PBE functional was employed to describe the system. Within the framework of Gaussian wave and plane wave methods, Kohn-Sham density functional theory (DFT) was utilized as the electronic structure method. The integration time step was set to 1 fs. The temperature was maintained at 298 K using the NPT ensemble. The radial distribution functions were analyzed using the VMD software package.

Supplementary Figures

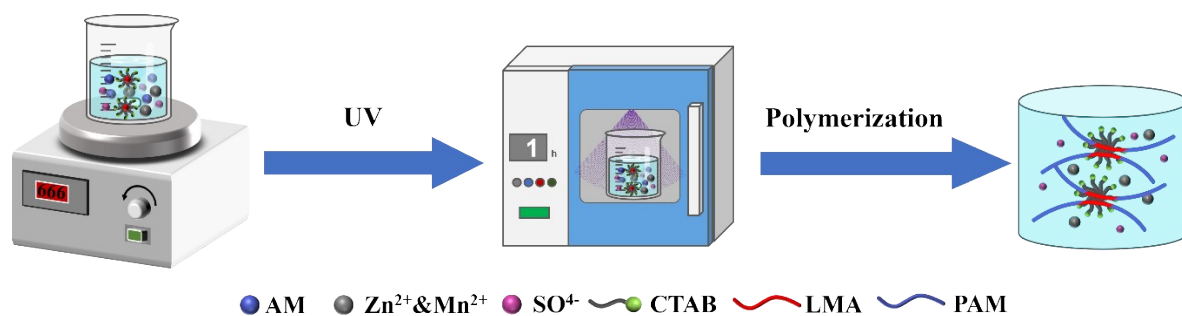


Figure S1. Preparation flow chart of LA gel electrolytes.

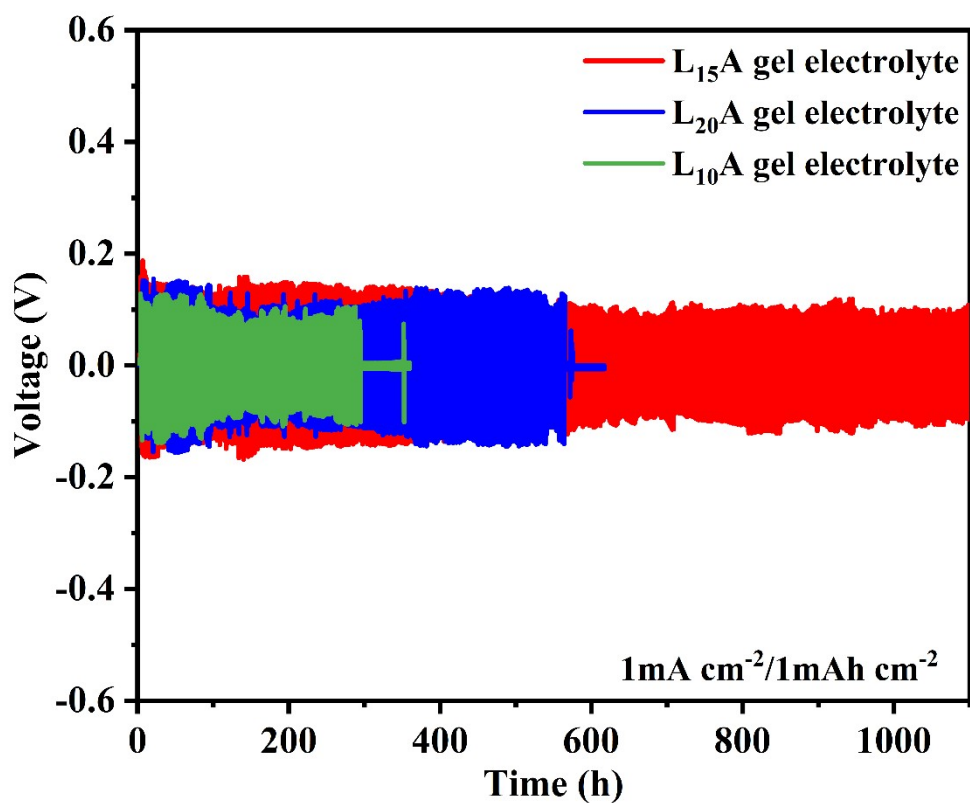


Figure S2. Cycling performance of Zn||Zn symmetric cells at 1 mA cm⁻²/ 1 mAh cm⁻² with different electrolytes.

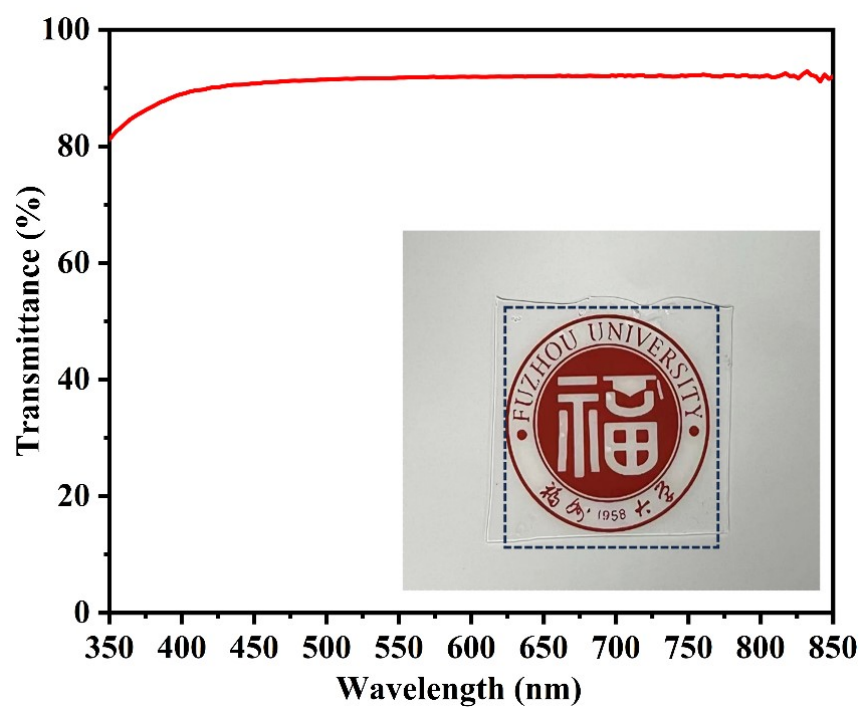


Figure S3. UV-Vis transmittance of L₁₅A gel electrolyte and the photograph showing its transparency.

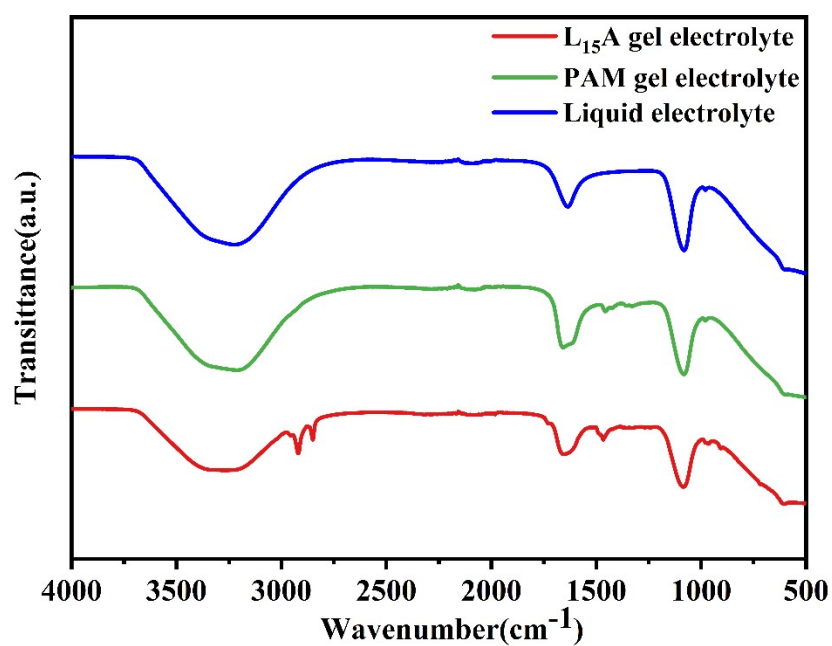


Figure S4. FT-IR spectra.

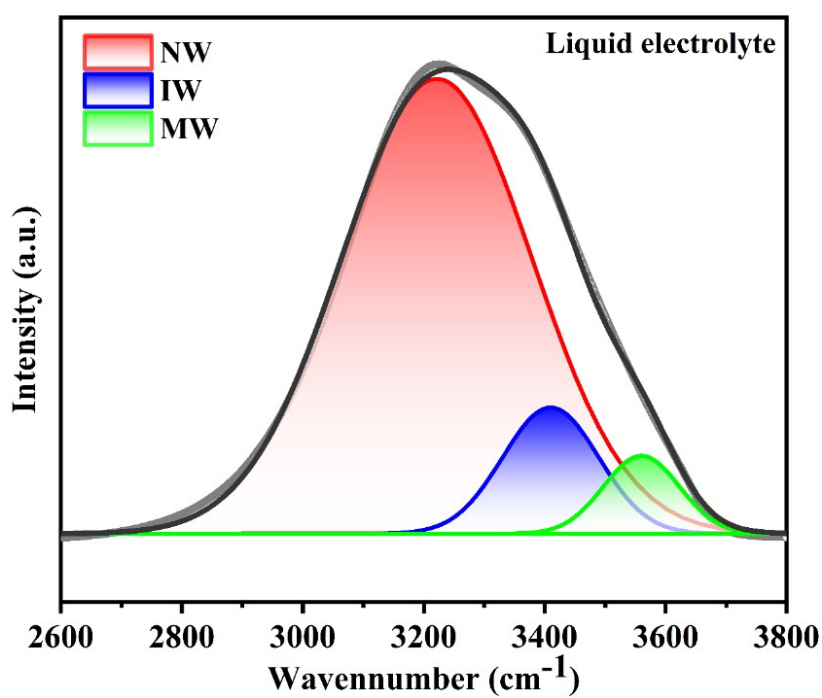


Figure S5. Related curve fitting results of the liquid electrolyte.

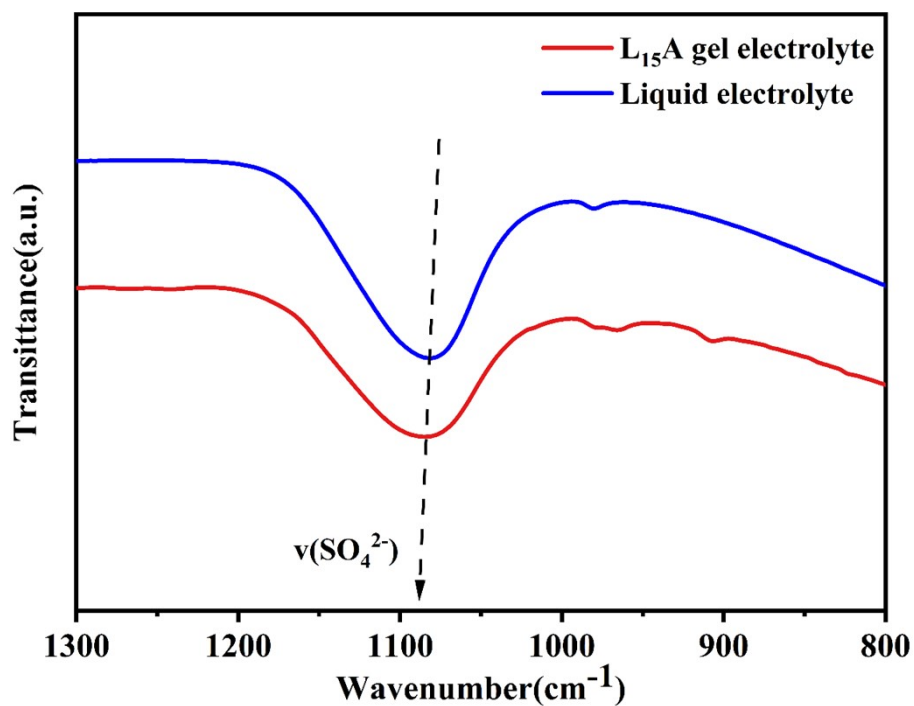


Figure S6. FTIR spectra of liquid and L15A gel electrolytes in a selected range.

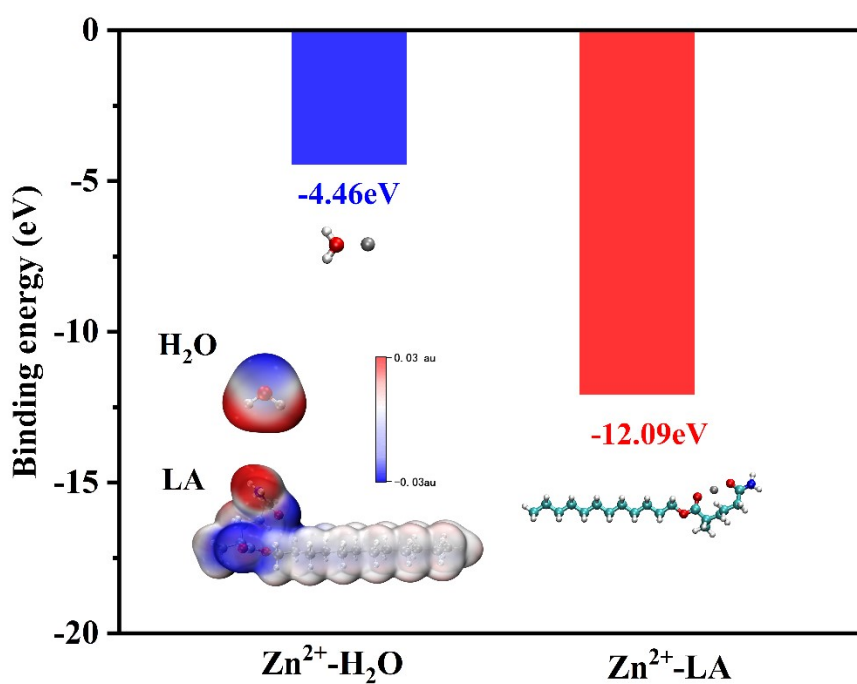


Figure S7. Binding energy of Zn^{2+} with LA and H_2O , the inset shows ESP mappings of LA and H_2O .

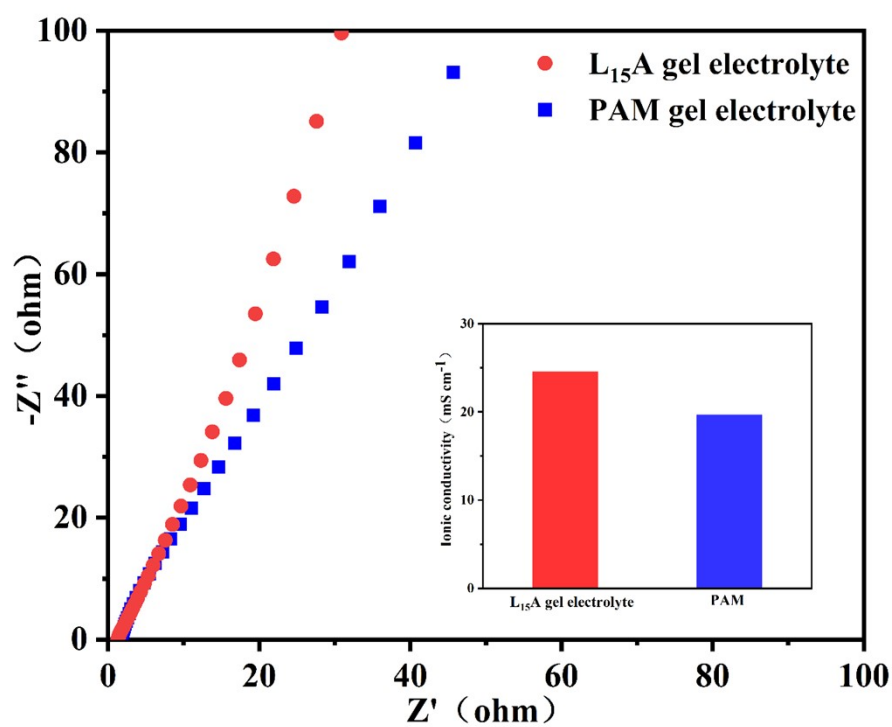


Figure S8. Ionic conductivities of the $L_{15}A$ gel electrolyte and PAM gel electrolyte.

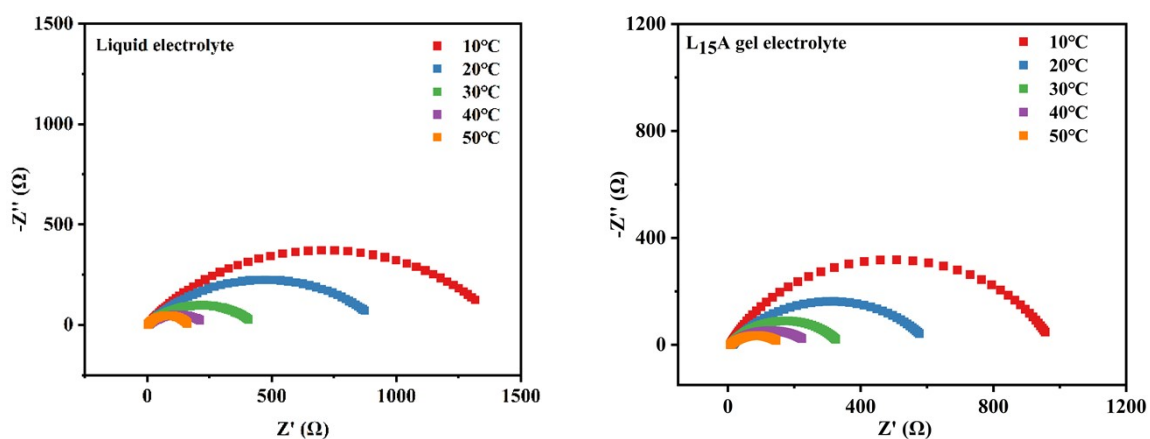


Figure S9. Nyquist plots of Zn//Zn symmetric cells testing under various temperatures in (a) the liquid electrolyte and (b) the L₁₅A gel electrolyte.

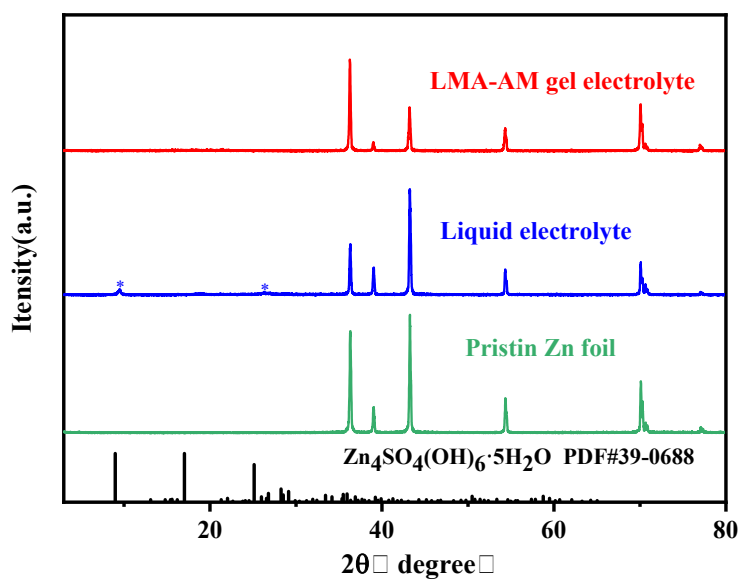


Figure S10. XRD pattern of the Zn deposition surface after 50 cycles.

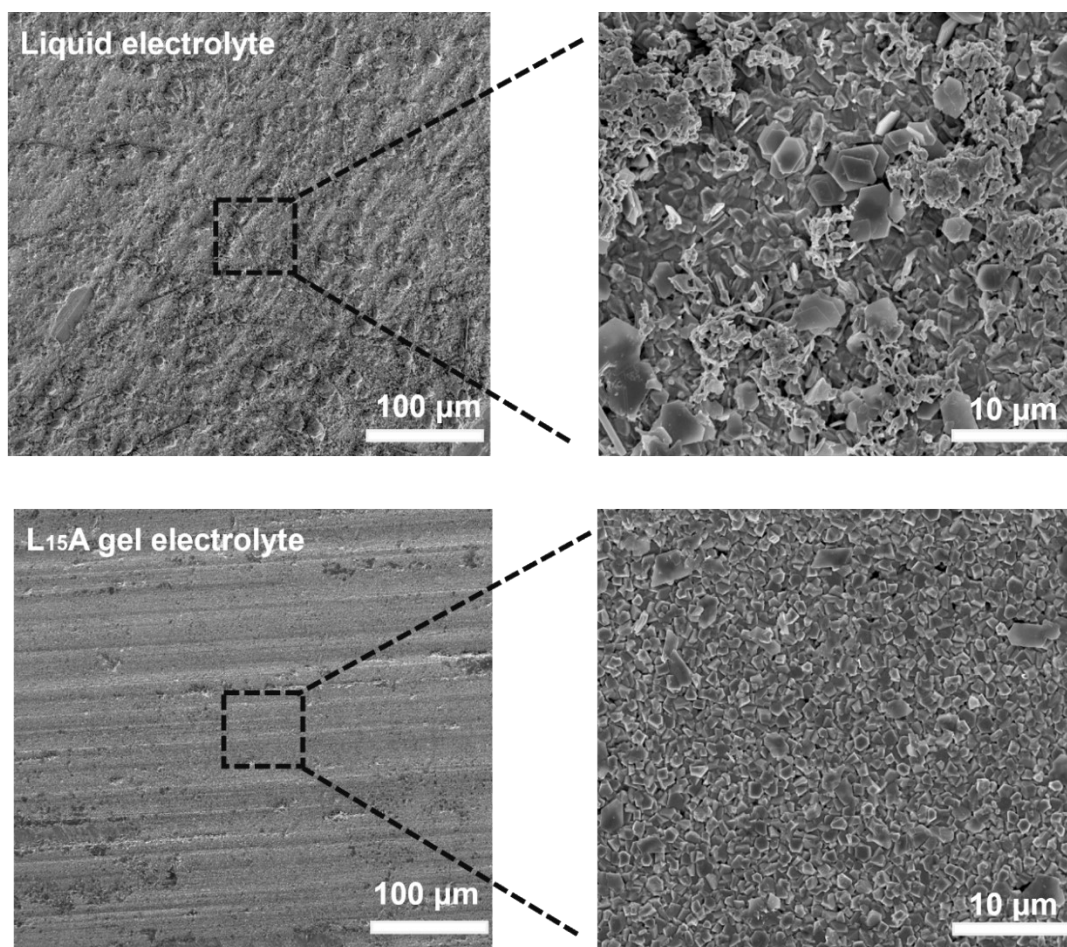


Figure S11. SEM images of the Cu substrate after 50 cycles of Zn||Cu battery using different electrolytes at 1 mA cm^{-2} .

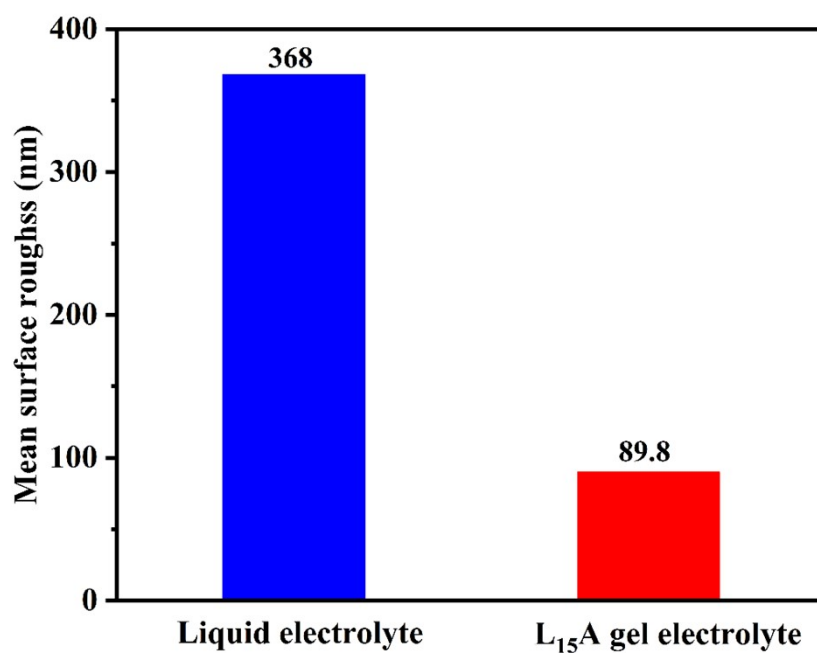


Figure S12. The mean surface roughness (Ra) of AFM images for different

electrolytes.

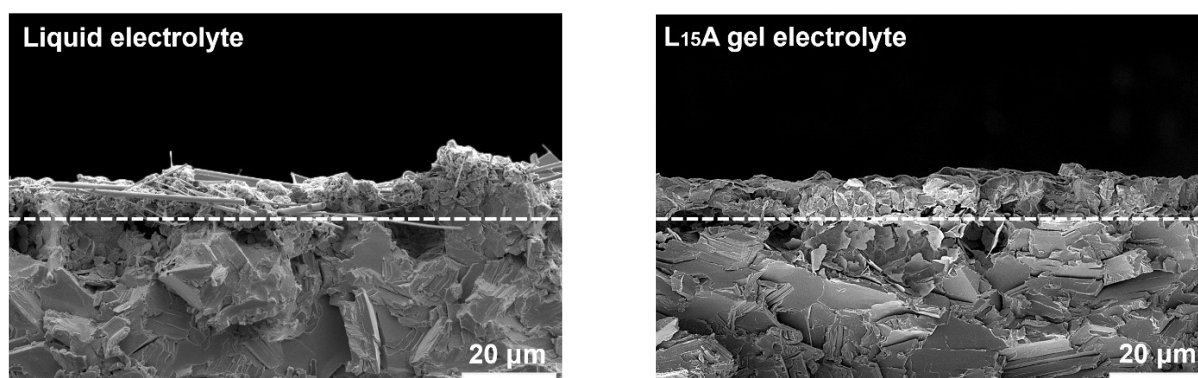


Figure S13. The cross-sectional SEM images of the Zn foils after 50 cycles at $1\text{mA cm}^{-2}/1\text{mAh cm}^{-2}$

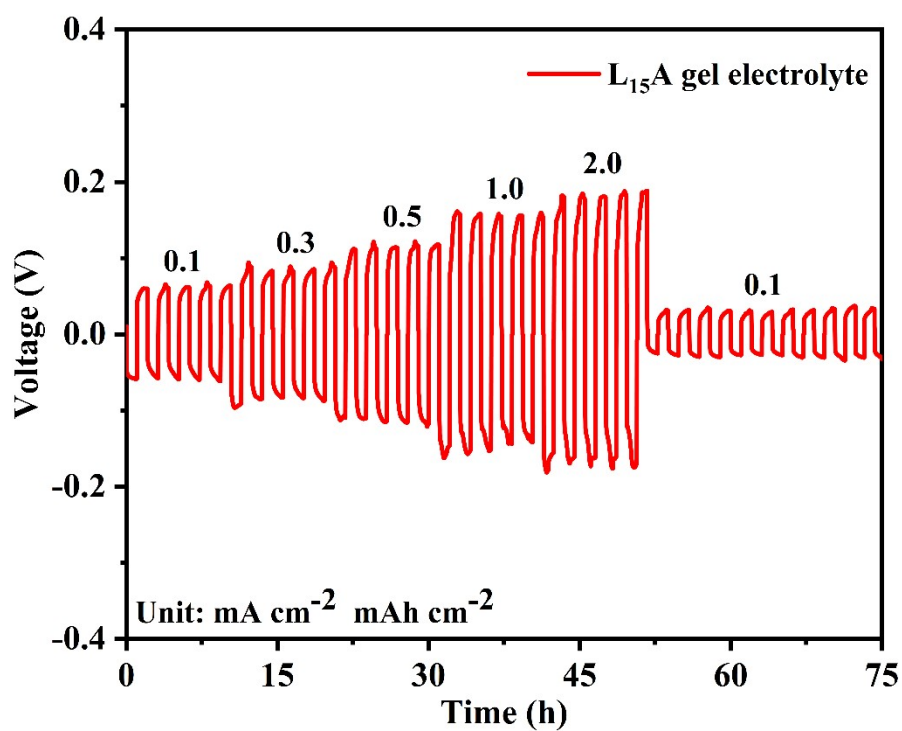


Figure S14. Rate performance of Zn||Zn symmetric cell with L₁₅A gel electrolyte.

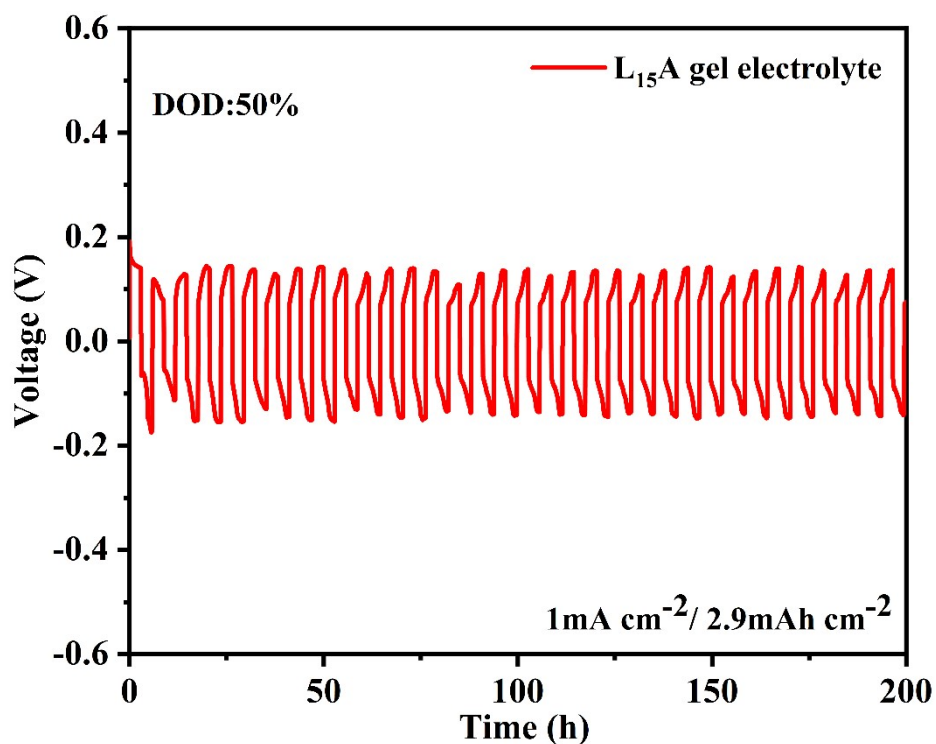


Figure S15. Cycling performance of Zn||Zn symmetric cells at $1 \text{ mA cm}^{-2} / 2.9 \text{ mAh cm}^{-2}$ (DOD=50%) .

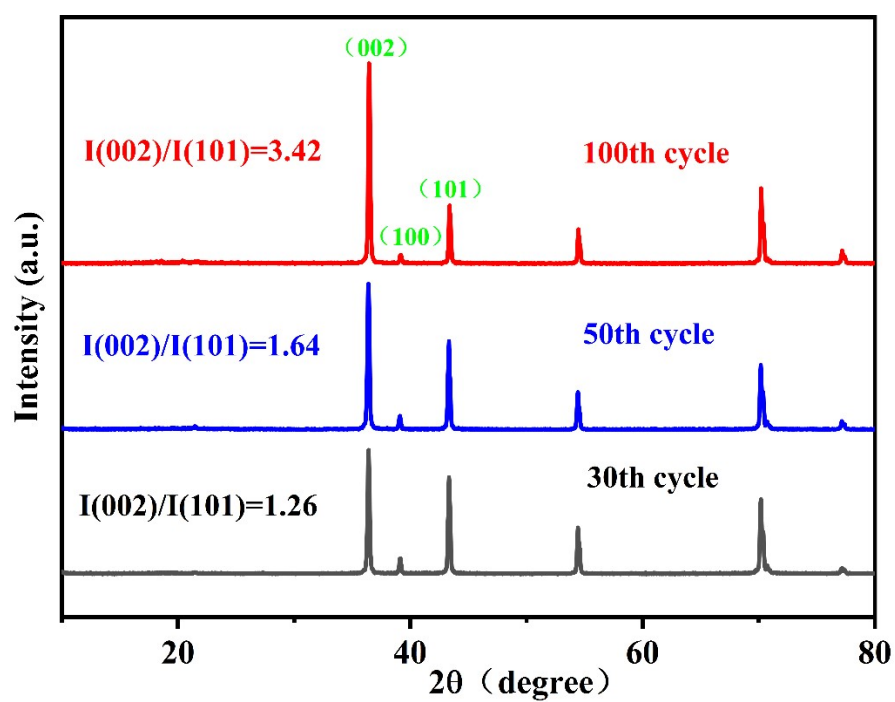


Figure S16. XRD patterns of Zn foils in symmetrical cells with $L_{15}A$ gel electrolyte after 50 cycles.

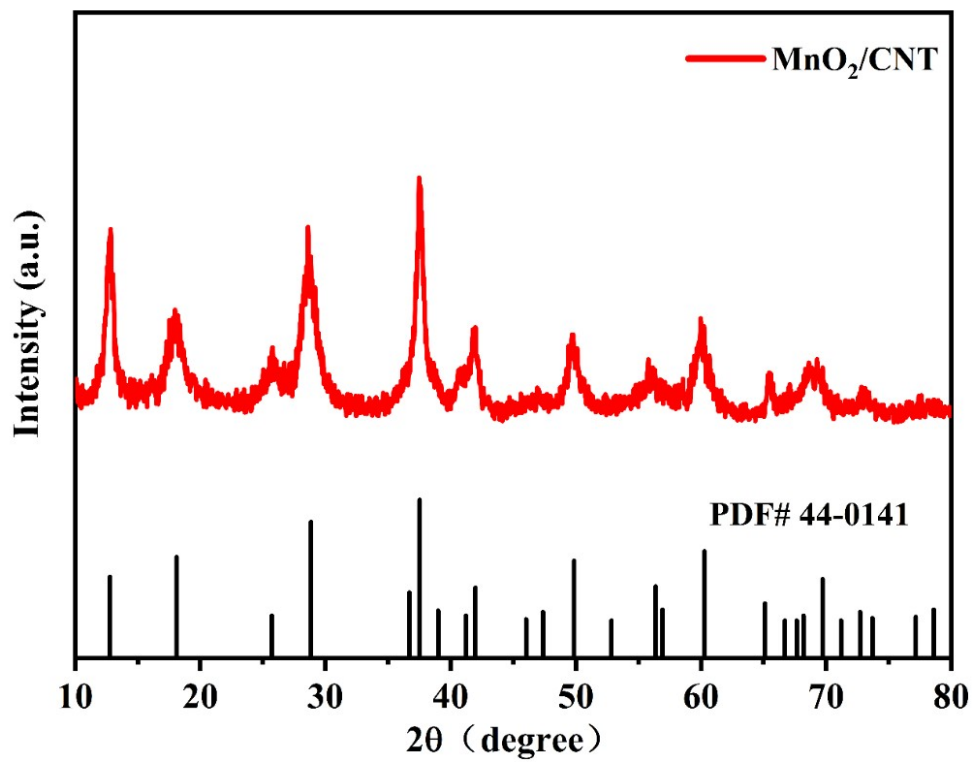


Figure S17. XRD pattern of MnO₂/CNT sample.

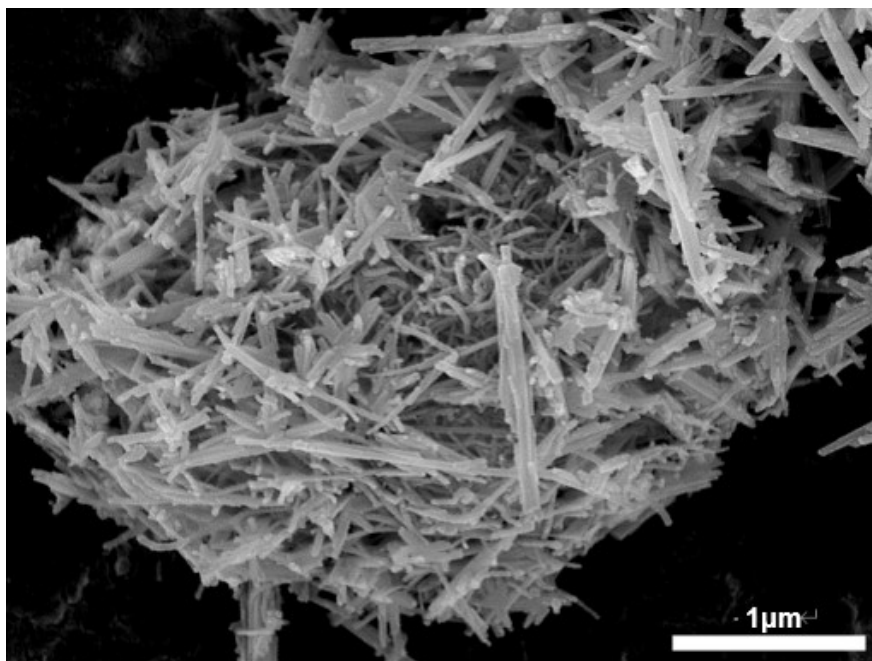


Figure S18. SEM image of the MnO₂/CNT sample.

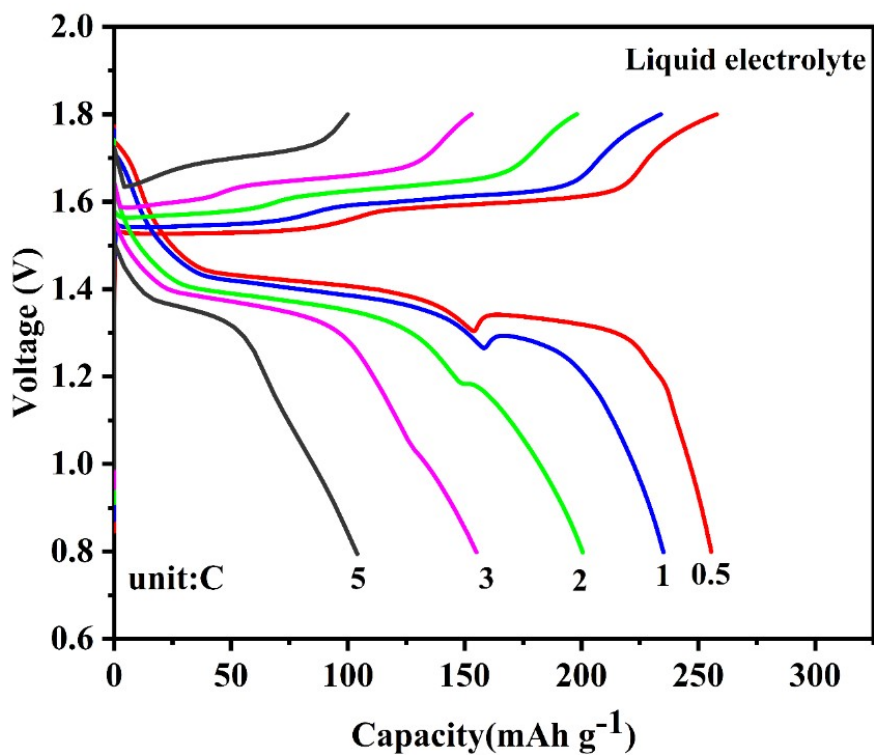


Figure S19. Charge-discharge curves under different rates with liquid electrolyte.

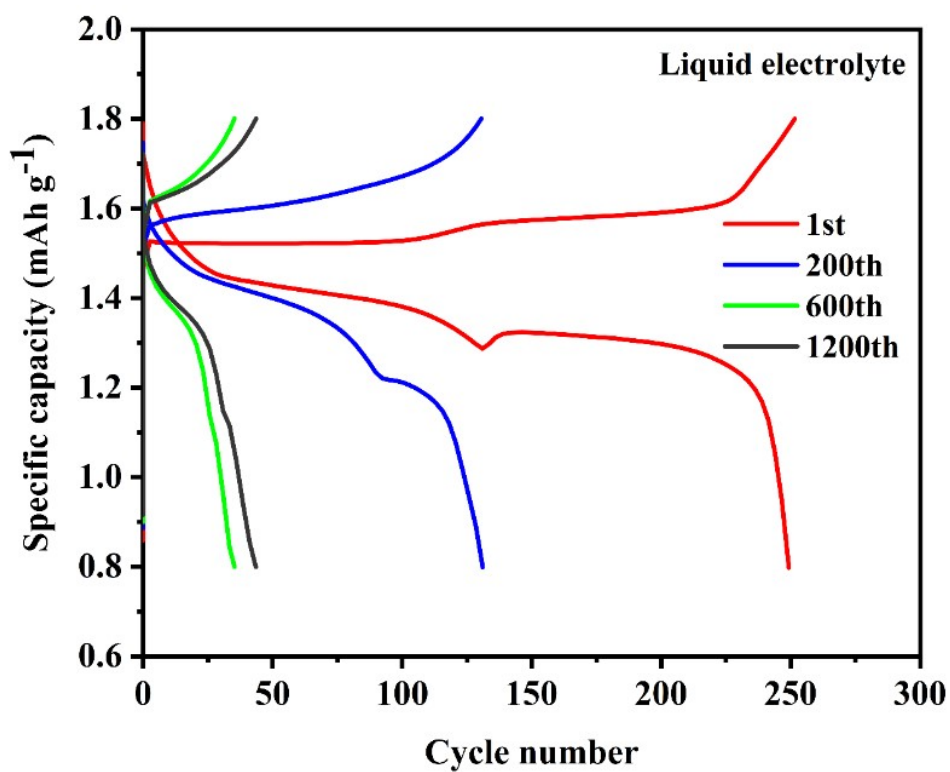


Figure S20. Charge-discharge curves under 1C at different cycle numbers with liquid electrolyte.

Table S1. Electrochemical performance and Zn utilization of different electrolytes.

Thickness of Zn foil (μm)	Cycling performance ($\text{mA cm}^{-2}/\text{mAh cm}^{-2}/\text{lifespan}$)	Zn utilization	References
10	1 $\text{mA cm}^{-2}/2.9 \text{ mAh cm}^{-2}/200\text{h}$	50%	This work
100	1 $\text{mA cm}^{-2}/0.5 \text{ mAh cm}^{-2}/750\text{h}$	8.5%	25
30	1 $\text{mA cm}^{-2}/5 \text{ mAh}/700\text{h}$	28.4%	37
20	5 $\text{mA cm}^{-2}/5 \text{ mAh cm}^{-2}/160\text{h}$	42.7%	38
60	1 $\text{mA cm}^{-2}/5 \text{ mAh cm}^{-2}/800\text{h}$	14.2%	39